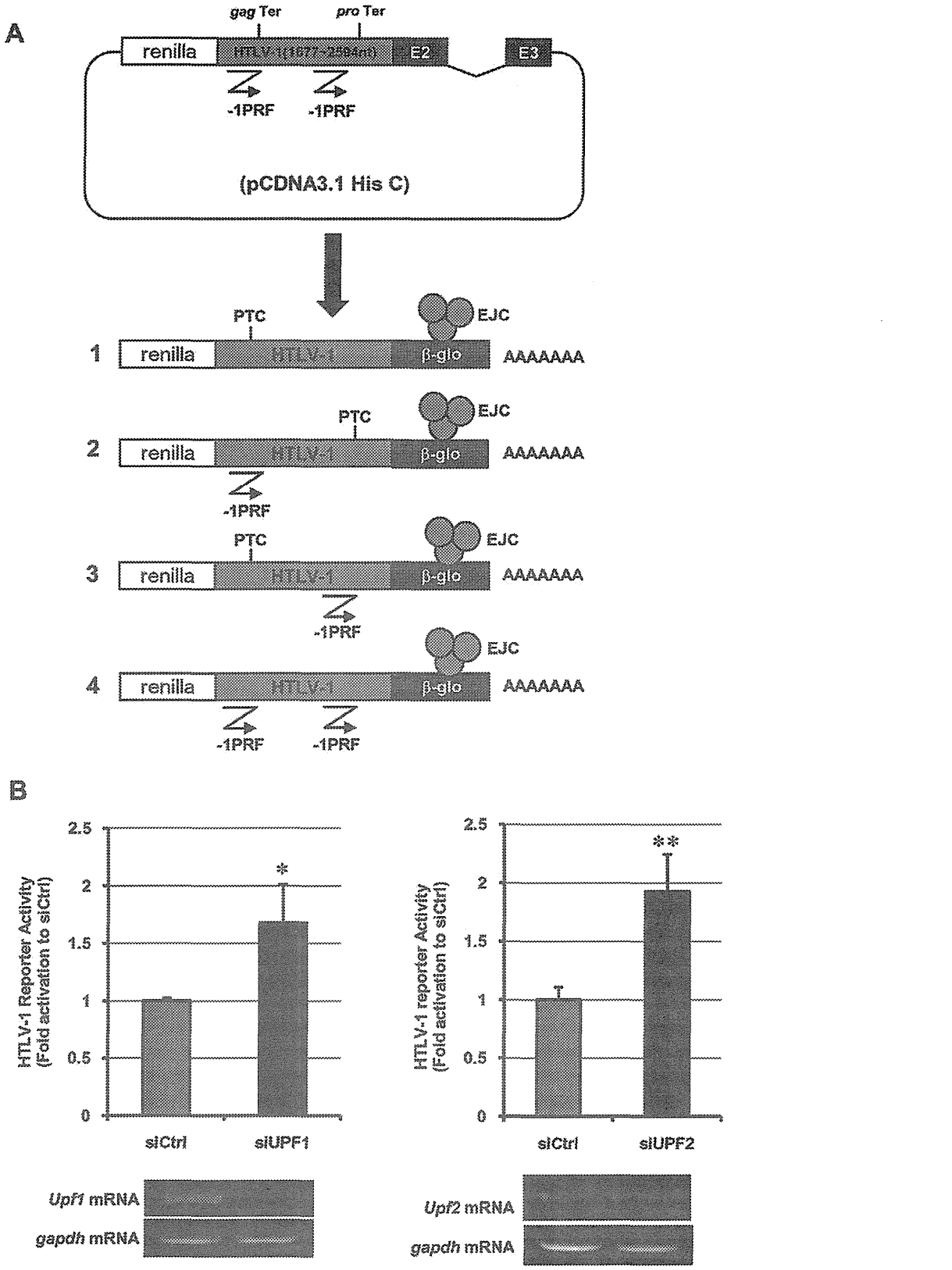

Fig. 2. HTLV-1 derived reporter activity is NMD sensitive. (A) A schematic structure of the HTLV-1 derived reporter plasmid and four possible translation patterns. As indicated, the HTLV-1 fragment in the reporter plasmid contains two −1 PRF signals (shown by ⩙) and 3/4 of these translation patterns result in PTC. (B) The HTLV-1 derived reporter activity was NMD dependent in HeLa cells. The relative HTLV-1 reporter activity was increased by NMD inhibition through siRNA-mediated suppression of UPF1 and UPF2 ($n = 3$–5, mean ± SD; $^{*}p < 0.05$; $^{**}p < 0.01$).

infection but not to contamination of co-cultured MT-2 cells (for genomic fingerprinting PCR, see Supplementary material and methods for more details) (Fig. S2B). NMD activity in these HTLV-I-infected sHeLa cells was significantly suppressed on day 1 ($p < 0.05$) and on day 2 ($p < 0.01$) after infection compared with that in control sHeLa cells co-cultured with uninfected cells (Fig. 3D). These results indicated that HTLV-1 caused a temporal suppression of NMD activity. Of note, the timing of maximum suppression of NMD activity corresponded to the peak expression of HTLV-1 *tax/rex* mRNAs and proteins and correlated with peak accumulation of HTLV-1 unspliced mRNA (Fig. 3C and D). Moreover, co-culture of sHeLa cells with MT-2 in the presence of the reverse transcriptase inhibitor azidothymidine (AZT) resulted in a dose-dependent rescue of NMD activity, supporting the idea that the suppression of NMD activity is indeed caused by HTLV-1 infection of target sHeLa cells and that this suppression requires reverse transcription and provirus integration (Fig. 3E).

3.5. HTLV-1 Rex is the principal viral factor inhibiting host NMD activity

Next, we examined HTLV-1 gene products for the ability to suppress host NMD activity. The relative NMD activity in sHeLa cells that ectopically express p27Rex (Rex), p21Rex, p30II, and Tax was analyzed using the dual-luciferase NMD reporter assay at 24,36, and 48 h after transfection. As shown in Fig. 4A, NMD activity was significantly suppressed 24 h after transfection when p27Rex or p21Rex was expressed. In these experiments, the HTLV-1 transcriptional transactivator Tax was also found to inhibit NMD activity, but this effect was consistently less than that observed for p27Rex or p21Rex.

The most significant impact on host NMD activity was the dose-dependent suppression exerted by p27Rex and to a slightly lesser degree, p21Rex (Fig. 4B). Of note, NMD reporter constructs do not contain sequences corresponding to the highly structured RxRE. Consequently, we suggest that the suppression of NMD activity by Rex is not due to RxRE-dependent and Rex-mediated nuclear export of unspliced mRNAs. Indeed, nuclear export of unspliced β-globin mRNA, transcribed from the reporter plasmid, was not enhanced by Rex (Fig. S3A). We also confirmed that insertion of RxRE after the β-globin sequence of the NMD reporter plasmid did not exhibit any significant influence on Rex-induced NMD inhibition (Fig. S3B). Moreover, our study demonstrated that p21Rex, which lacks the N-terminal RxRE-binding domain, also exhibited NMD inhibitory activity, supporting the view that NMD inhibition is due to a genetically separable aspect of Rex function that is independent of the arginine-rich RxRE-binding motif. Other HTLV-1 accessory proteins, such as p12, p13, and antisense-encoded HBZ, did not show any significant influence on the cellular NMD activity (Fig. S4).

3.6. Rex inhibits global NMD activity of the cell

On confirmation that Rex stabilizes chimeric NMD reporter mRNA, we tested if Rex stabilizes endogenous NMD target mRNA. Fig. 5 shows the decay rates of NMD target mRNAs in CEM cells stably expressing Rex or in control cells showing no Rex expression. The selected mRNAs contained uORFs (MAP3K14, IL6, DUSP10, Fyn, PTPRF, ARHGEF18, and ASNS) or 3′ UTR intron (DEXI) as NMD-inducing features and stabilization under UPF1 knockdown was confirmed (MAP3K14, PTPRF, ARHGEF18, and ASNS) or expected (DUSP10, Fyn, IL6, and DEXI) by Mendell et al. [2]. The graphs show that these mRNA substrates for NMD are significantly stabilized by Rex overexpression in a T cell line. These NMD target mRNAs were specifically stabilized in CEM-Rex, since the stability of β-actin mRNA, a non-NMD target, was almost the same between CEM-empty and CEM-Rex when the stabilities of β-actin mRNA and NMD target mRNA were separately illustrated (data not shown). These results provide strong evidence that Rex serves as a general inhibitor of NMD.

3.7. NMD inhibition by Rex enhances HTLV-1 expression

Finally, we examined the effects of p27Rex, p21Rex, p30II, and Tax on HTLV-1 derived reporter activity. As shown in Fig. 6A, p27Rex significantly increased HTLV-1 reporter activity, which was very similar to that following NMD inhibition by siUPF1 or siUPF2 (Fig. 2B). p21Rex also significantly elevated HTLV-1 reporter activity, but to a lesser extent compared with p27Rex, whereas p30II and Tax did not significantly influence reporter activity (Fig. 6A). As anticipated from the accrued data and early reports by others [18–20], we also demonstrated that unspliced HTLV-1 mRNA was significantly stabilized in cells containing p27Rex (half-life = 11.3 h) compared with control cells containing empty vectors (half-life = 2.3 h) (Fig. 6B). On the other hand, p30II and Tax did not show significant effects on stabilization of unspliced HTLV-1 mRNA (half-lives = 3.4 h and 2.8 h, respectively). Interestingly, p21Rex, which does not have NLS and hence does not localize to the nucleus, also stabilized unspliced HTLV-1 unspliced mRNA (half-life = 11.0 h). These data further support that stabilization of viral genomic RNA by Rex is, at least partially, achieved by its function in the cytoplasm. Significantly, viral particle production, as determined by HTLV-1 Gag p53 (precursor), p24, and p19 protein expression levels, was increased under conditions of NMD inhibition by antisense-*upf2* mRNA overexpression that suppressed UPF2 protein expression (Fig. 6C). In addition, this increased level of Gag protein, especially in p53 and p19, was comparable to that observed following p27Rex and p21Rex overexpression (Fig. 6D). Given that p27Rex and p21Rex significantly stabilizes HTLV-1 *gag* mRNA (Fig. 6B), these data suggest that Rex enhances HTLV-1 replication by stabilizing unspliced viral transcripts via the suppression of host NMD activity.

4. Discussion

In this study, we demonstrate that HTLV-1 genomic and *gag/pol* RNA is recognized by UPF1, the principal regulator and initiator of NMD, and is thereby targeted for destruction

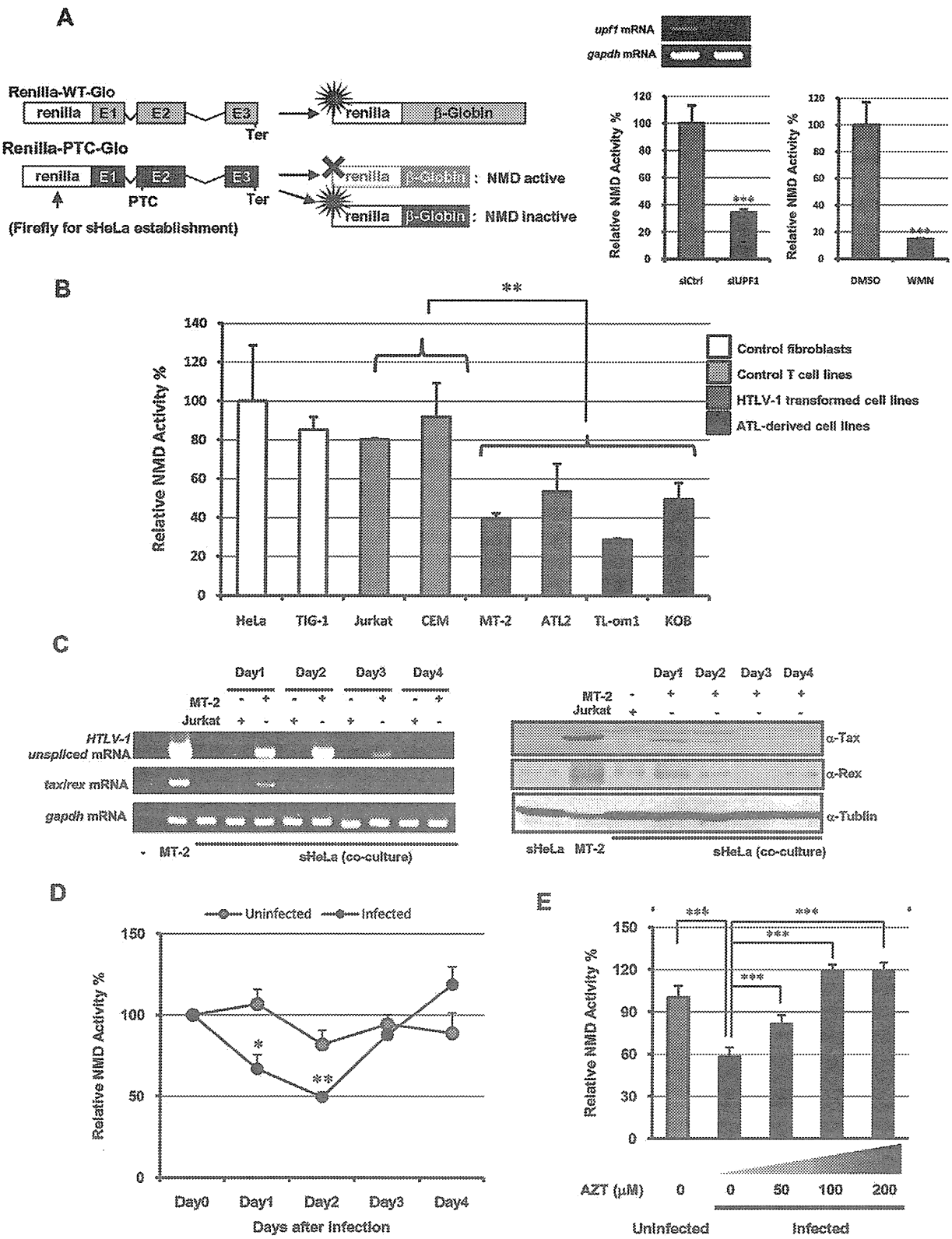

Fig. 3. HTLV-1 infection inhibits cellular NMD activity. (A) A schematic representation of the β-globin NMD reporter plasmids. PTC indicates a premature termination codon and Ter indicates a WT stop signal. The renilla fragment of Renilla-PTC-Glo was replaced with the firefly fragment for establishment of sHeLa cells, which stably expressed both Renilla-WT-Glo and Firefly-PTC-Glo, thus WT-Glo and PTC-Glo expression level was detected as renilla and firefly luciferase activity, respectively. ✸ indicates the luciferase activity. The renilla activity of Renilla-WT-Glo is always active and not influenced by the cellular NMD activity.

by the host NMD machinery. Moreover, we found that HTLV-1 has evolved mechanisms to override and escape the host NMD pathway. We provide evidence that HTLV-1 Rex plays a critical role in the suppression of host NMD activity.

Firstly, we demonstrated that the host-encoded NMD specifically targets HTLV-1 genomic RNA and primary transcripts for RNA turnover. Therefore, host NMD acts to reduce viral structural gene expression and perturbs virus production. The steady-state expression of HTLV-1 unspliced mRNA showed a negative correlation with cellular NMD activity (Fig. 1A), and the stability of unspliced viral mRNA was highly sensitive to cellular NMD activity (Fig. 1B). Luciferase reporter assays, in which the luciferase activity reflects the stability of a *gag*-derived fragment of HTLV-1 genomic RNA, showed that the stability of HTLV-1 *gag* mRNA was directly influenced by the cellular level of UPF1 or UPF2, the key positive regulator of NMD (Fig. 2). Many researchers have demonstrated that UPF1 phosphorylation by the serine/threonine kinase SMG1 facilitates triggering of NMD and exclusion of aberrant mRNAs from the normal translational pathway. These mRNAs are redirected to the P-body, where they await targeted turnover [21,22]. UPF1 plays an important role in discrimination of PTCs that are positioned upstream of EJC at the last exon–exon boundary of spliced mRNAs and selectively activates the NMD machinery for degradation of the targeted mRNA [23]. Recognition of PTC by UPF1 is achieved by interaction of UPF1 at the termination codon with UPF2/UPF3 at EJC, which becomes possible only when a termination codon is positioned upstream of EJC. In yeast, the P-body is the major site for PTC-containing aberrant mRNAs awaiting degradation [24–26]. In mammalian and human cells, all NMD components localize to P-bodies [21] and phosphorylated UPF1 accumulates at these structures [22], supporting the notion that P-bodies accumulate mRNAs targeted for NMD turnover in mammalian cells. Taken together, accumulating evidence indicates that UPF1 is the key regulator in discrimination, selection, and translocation of aberrant mRNAs to P-bodies where they await degradation [21–23,26,27]. The results in the present study demonstrate that phosphorylated UPF1 interacts with HTLV-1 unspliced RNA with a high affinity and the HTLV-1 unspliced RNA complex accumulates in P-bodies (Fig. 1C and D). Our results thus indicate that HTLV-1 genomic RNA is detected by UPF1 as are other cellular NMD target mRNAs and transferred to P-bodies for degradation. Consistent with this notion, NMD antagonized efficient HTLV-1 replication (Fig. 1A and B), whereas the suppression of NMD activity led to a significant increase in HTLV-1 Gag proteins, p53, p24, and p19 (Fig. 6C). Thus, NMD destabilizes HTLV-1 genomic RNA and reduces the expression of viral structural proteins, presumably leading to a reduction in viral particle formation.

Several reports raise the possibility that retroviral transcripts are selectively targeted by the host mRNA decay mechanism, and they have unique or overlapped strategies to avoid degradation. Viral mRNAs of Rous sarcoma virus (RSV) [28] and human foamy virus [29] are selectively degraded in the host cell, although the authors of those studies concluded that the degradation may be accomplished by pathways distinct from NMD. Ajamian et al. reported influence of host encoded NMD-factor, UPF1, on unspliced HIV-1 mRNA, intriguingly enhancing the stability of HIV-1 mRNA [30]. Hogg and Goff proposed a possible model that 3′ UTR-length-dependent accumulation of UPF1 functions as a mark of potential mRNA-decay target [31]. The authors speculated that retroviruses may take advantage of this host-encoded system by employing in-frame read though and/or frame-shifting, which prevents steady-state UPF1 interaction and RNP composition, thus disrupts recognition of the viral mRNA as a decay target. In addition to these previous reports, our data show that unspliced HTLV-1 RNA is a target of a powerful host-encoded mRNA decay mechanism, NMD, and for efficient replication and propagation of new viral particles, it is critical for HTLV-1 to evade the NMD pathway.

On confirming that the host NMD pathway represents a significant impediment to efficient HTLV-1 replication, we posed the critical question: has HTLV-1 evolved a strategy to evade NMD? We observed that HTLV-1-infected cell lines have significantly lower basal NMD activities than HTLV-1-unrelated cell lines (Fig. 3B), implying that HTLV-1 infection may influence host NMD activity. Indeed, the NMD activity was notably suppressed by HTLV-1 infection or protected by inhibition of HTLV-1 infection via AZT treatment (Fig. 3C–E), suggesting the existence of viral factor(s) that suppress the host NMD pathway. Besides the structural proteins, HTLV-1 encodes regulatory and accessory proteins (Tax, Rex, p30II, p12, and p13) in the pX region of the genome. The functions of those proteins have been well studied and reviewed [32,33]. Tax is a multifunctional oncoprotein and transcriptional transactivator that regulates both viral and cellular gene expression [34,35]. HTLV-1 Rex is a virus-encoded, high-affinity, RNA-binding protein that binds

On the other hand, the luciferase activity of PTC-Glo, of which transcript is NMD target, can be detected only under NMD inhibition. The reporter is sensitive to changes in NMD activity in HeLa cells (right panel). Data from three independent experiments are shown ($n = 3$, mean ± SD; $^{***}p < 0.001$). (B) NMD activities were measured by β-globin-based NMD reporter assays in control fibroblasts (HeLa and TIG-1), control T-cell lines (Jurkat and CEM), HTLV-1-transformed cell lines (MT-2 and ATL2), and ATL-derived cell lines (TL-Om1 and KOB). HTLV-1-infected T cell lines show significantly lower NMD activities compared with HTLV-1-unrelated cell lines. Data from three independent experiments are shown ($n = 3$, mean ± SD; $^{**}p < 0.01$). (C) The course of HTLV-1 expression in sHeLa cells co-cultured with MT-2. *Gag* or *tax/rex* mRNA by RT-PCR (left panel) as well as Tax and Rex protein levels determined by Western blotting (right panel) show peaked viral expression 1 and 2 days after infection. (D) NMD activity was measured via dual luciferase assays in HTLV-1 infected sHeLa cells and compared with that in uninfected control cells. Gray circles indicate the results from uninfected control cells, while black circles represent data from HTLV-1 infected cells. Significant NMD inhibition was observed on the first ($p < 0.05$) and second ($p < 0.01$) days after HTLV-1 infection. Results shown are from three independent experiments ($n = 3$, mean ± SE; $^{*}p < 0.05$; $^{**}p < 0.01$). (E) NMD inhibitory effect of HTLV-1 infection is diminished by AZT treatment in HTLV-1 infected sHeLa cells by co-cultivation with MT-2 cells. NMD inhibition by HTLV-1 was abrogated in a dose-dependent manner by AZT treatment ($n = 6$, mean ± SD; $^{***}p < 0.001$).

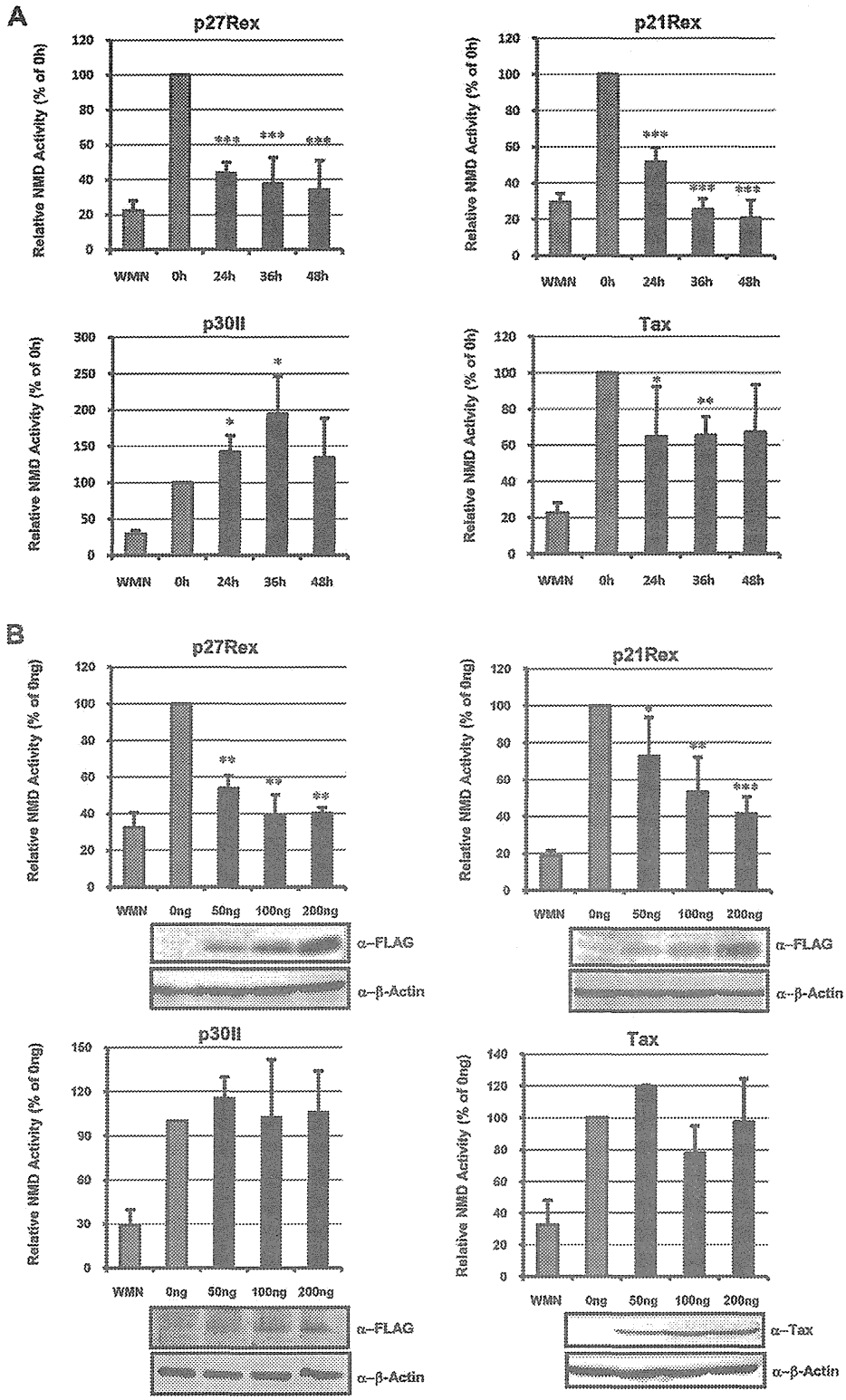

Fig. 4. HTLV-1 Rex is the key viral factor inhibiting NMD. (A) p27Rex and p21Rex inhibit NMD activity in a time-dependent manner, when 200 ng each of viral protein expression plasmid was transfected to sHeLa cells. Tax also demonstrated an NMD inhibitory effect but to a less significant level compared with p27Rex and p21Rex. A representative result from three independent experiments is shown ($n = 3$, mean ± SD; $^{*}p < 0.05$; $^{**}p < 0.01$; $^{***}p < 0.001$). (B) Both p27Rex and p21Rex suppressed NMD activity in a dose-dependent manner when 50–200 ng of viral protein expression plasmid was transfected to sHeLa cells. A representative result from three independent experiments is shown ($n = 3$, mean ± SD; $^{*}p < 0.05$; $^{**}p < 0.01$; $^{***}p < 0.001$).

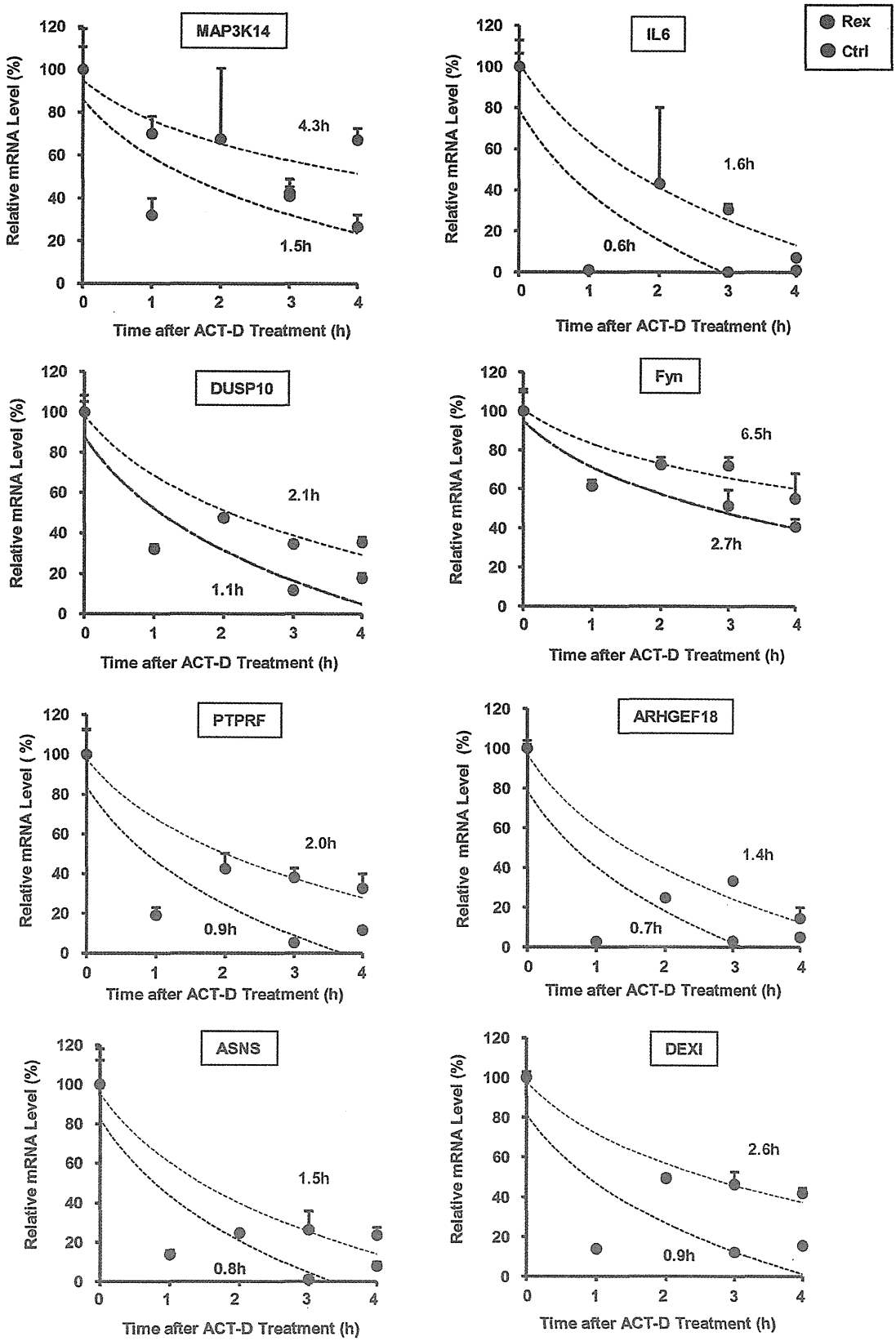

Fig. 5. Rex inhibits global NMD activity. The stability of NMD target mRNAs containing uORFs or 3′ UTR introns as NMD-inducing features [2] were measured in CEM-Rex and CEM-Ctrl. These mRNAs for NMD substrates were significantly stabilized in Rex-overexpressing cells, indicating that Rex represents a general block to global cellular NMD activity. Red circle: CEM-Rex; black circle: CEM-Ctrl. The indicated time is the half-life of tested mRNA calculated based on the regression curve (dashed line).

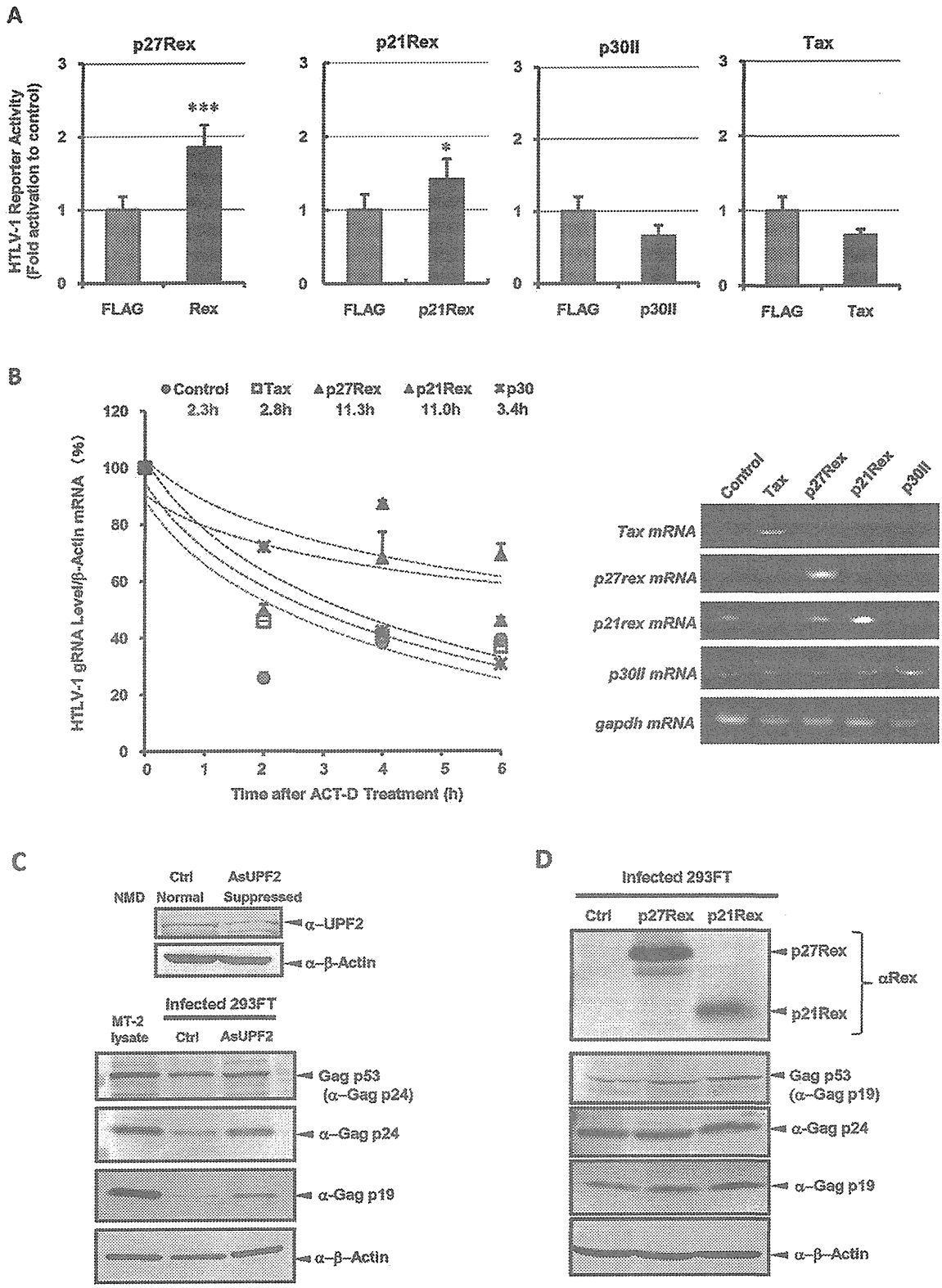

Fig. 6. Rex stabilizes HTLV-1 unspliced mRNA and enhances viral replication via NMD inhibition. (A) The effects of p27Rex, p21Rex, p30II, and Tax on HTLV-1 derived reporter activity in HeLa cells. The reporter activity was significantly increased by p27Rex and p21Rex but not by p30II and Tax ($n = 3–5$, mean ± SD; $^{*}p < 0.05$; $^{***}p < 0.001$). (B) The effect of HTLV-1 regulatory proteins p27Rex (red ▲), p21Rex (purple ▲), p30II (black×), Tax (blue□), and control (green●) on the stability of HTLV-1 genomic unspliced RNA in HTLV-1 infected HeLa cells by co-cultivation with MT-2 cells. HTLV-1 unspliced RNA in p27Rex-overexpressing cells was significantly stabilized (half-life = 11.3 h), followed by stabilization in p21Rex-overexpressing cells (half-life = 11.0 h) compared

to the Rex response element (RxRE) of viral transcripts and promotes selective nuclear export of viral genomic RNA [32,36]. P30II is also an RNA-binding protein that binds mainly to double-spliced *tax/rex* mRNA and reduces translation from this mRNA by retaining it to the nucleolus [37–39]. In a series of experiments testing the influence of these viral factors on NMD activity, only p27Rex and p21Rex displayed a robust time- and dose-dependent inhibition of NMD activity (Fig. 4). The most important and well-studied function of Rex is to promote nuclear export and enhance the stability of unspliced and singly spliced HTLV-1 mRNAs that encode viral structural proteins, by interacting with Rex Responsive Element (RxRE) situated at the 3′ end of all HTLV-1 mRNAs [18,19,40–42], and by engagement with the cellular nuclear export factor CRM1 [18,43,44]. The molecular mechanism of Rex in protection of unspliced viral RNA has not been fully clarified, however, partially explained by active export of mRNA from the nucleus, thereby escaping from the site of splicing. Nevertheless, the fate of viral RNA in the cytoplasm has not been methodically explored. From our data, we propose that Rex assists viral RNA transit within the cytoplasm and ensures efficient translation by subduing NMD and the host mRNA surveillance systems.

We demonstrated that the NMD activity of TL-Om1 cells was significantly suppressed (Fig. 3B), although these cells do not express any of viral proteins at detectable levels. The molecular mechanism of NMD inhibition in TL-Om1 cells is apparently different from that of Rex expressing cells, however, it can be conceived that disturbances of cellular homeostasis caused by HTLV-1 during the early stages of infection, including inhibition of NMD by Rex, might have been conserved after malignant transformation of the infected cells. To gain further insights into the mechanisms, comparative analyses of cell lines that were HTLV-1 immortalized in vitro, such as MT-2, and those derived from ATL and without Rex expression, such as TL-Om1, may provide valuable information as model cells in the early stages of infection and immortalization, and those in the later transformed phase, respectively.

During the completion of our study, Mocquet et al. [45] demonstrated that HTLV-1 Tax interacts with UPF1 and exerts an inhibitory effect on NMD activity. In the present study, Tax also consistently exhibited an inhibitory effect on NMD activity, but both p21Rex and p27Rex consistently outperformed Tax in our assays (Figs. 4 and 6A). Therefore, the studies described here specifically focused on the inhibition of NMD activity exerted by both Rex alleles. In our view, it is not surprising that retroviruses have evolved multiple and overlapping mechanisms to overcome the restrictive properties of NMD. This is especially relevant at early times of viral infection or alternatively, when the provirus is emerging from latency. Under such conditions, there may be insufficient Rex concentration to saturate the NMD pathway. Therefore, another mechanism that augments the NMD inhibitory activity of Rex, such as that presented by Tax, may be required to cooperatively incapacitate NMD. Significantly, recent studies have demonstrated that *tax/rex* mRNAs are the most abundant viral transcripts at early times of infection or following proviral reactivation, and that viral gene expression follows a two-phase pattern that is determined principally by Rex [46].

Our data are consistent with the view that increased luciferase activity of NMD-sensitive reporters by Rex was due to the suppression of overall cellular NMD activity but not due to RxRE-mediated nuclear export of reporter mRNAs by Rex. This is because (1) none of the NMD reporter mRNAs used in this study contain RxRE; (2) the amounts of unspliced and spliced forms of β-globin mRNA in nuclear and cytosolic fractions of the cells were not influenced by Rex expression (Fig. S3A); and (3) the insertion of RxRE after the β-globin fragment of the NMD reporter plasmids had no impact on the NMD inhibitory effect of Rex (Fig. S3B). The data that p21Rex, lacking NLS and RxRE-binding domain at the N-terminal region, is also capable of suppressing NMD strongly support the notion that NMD inhibition is genetically separable from the RxRE-binding function of Rex (Fig. 4). Indeed, we demonstrated that Rex stabilizes a series of NMD target mRNA with NMD-inducing features such as uORFs and 3′ UTR introns (Fig. 5), providing strong evidence that Rex blocks overall cellular NMD activity. On the other hand, it is widely accepted that NMD is involved in cellular homeostasis not only by eliminating PTC-containing aberrant mRNAs but also by controlling the levels of natural transcripts. Approximately 1–10% of eukaryotic transcripts are known to be targeted by NMD because of their potentially NMD-sensitive structures, i.e., PTCs encoded by alternative exons, introns in 3′ UTRs, or uORFs [2,47]. Thus, NMD dysfunction can lead to the destruction of cell homeostasis and may even trigger tumorigenesis [48]. Clearly, overall NMD inhibition by Rex is beneficial to HTLV-1 as a direct mechanism to enhance the stability of HTLV-1 genomic RNA. In contrast, it may perturb cellular gene expression and discrimination of aberrant mRNAs, which are critically regulated by NMD under normal conditions. Indeed, NMD targets many mRNAs, of which products participate in cell cycle regulation, T cell

with that in control cells (half-life = 2.3 h). In contrast, Tax and p30II did not significantly stabilize HTLV-1 unspliced RNA (half-lives = 2.8 and 3.4 h, respectively). The half-life was calculated based on the regression curve (dashed line) (n = 4, mean ± SE). The right side panel shows mRNAs levels of *tax*, *p27rex*, *p21rex*, and *p30ii* at 0 h measured by semi-quantitative RT-PCR in HTLV-1 infected cells expressing the indicated viral proteins, ectopically. (C) Expression of HTLV-1 structural proteins, Gag p53 (precursor), p24, and p19, in HTLV-1 infected 293FT cells co-cultured with MT-2 after NMD suppression by As-*upf2* mRNA overexpression to knockdown UPF2 protein expression (top panel). The expression levels of all Gag proteins, p53, p24, and p19, were significantly elevated in the 293FT cells after NMD suppression. (D) The influence of p27Rex and p21Rex on the expression of HTLV-1 Gag structural proteins, p53, p24, and p19, in HTLV-1 infected 293FT cells co-cultured with MT-2. The results showed that the expression levels of HTLV-1 Gag proteins, especially those of Gag p53 and p19, were significantly increased by p27Rex and p21Rex overexpression.

development, and inflammation [2]. The potential pleiotropic impact of Rex mediated through the NMD pathway represents an important and novel aspect of host–retrovirus interaction in viral leukemogenesis.

In conclusion, this study provides evidence that the host-encoded NMD pathway restricts viral RNA expression, thereby reducing HTLV-1. Furthermore, we demonstrated that a novel function for HTLV-1 Rex in inhibition of the host NMD machinery. Rex-mediated inhibition of NMD activity is pleiotropic and may affect both viral and cellular target RNA. Together with the data presented here, there is accumulating evidence of a dynamic interplay between the cellular NMD pathway and pathways for viral gene expression and replication. Clarifying underlying molecular mechanism in inhibition of NMD by Rex is essential to understand this new aspect of host–pathogen interaction. Finally we suggest that the NMD pathway may exert anti-viral effects on other RNA viruses and may participate generally in the innate immune response to viral pathogens. It is therefore likely that other viruses have evolved mechanisms to silence NMD activity during viral infection.

Acknowledgment

This work was supported by Grants-in-Aid for Scientific Research from the Ministry of Education, Culture, Sports, Science, and Technology of Japan, to TW (No. 19659241) and to KN (Nos. 22700863, 24501304).

Appendix A. Supplementary data

Supplementary data related to this article can be found at http://dx.doi.org/10.1016/j.micinf.2013.03.006.

References

[1] R.T. Hillman, R.E. Green, S.E. Brenner, An unappreciated role for RNA surveillance, Genome Biol. 5 (2004) R8.
[2] J.T. Mendell, N.A. Sharifi, J.L. Meyers, F. Martinez-Murillo, H.C. Dietz, Nonsense surveillance regulates expression of diverse classes of mammalian transcripts and mutes genomic noise, Nat. Genet. 36 (2004) 1073–1078.
[3] F.J. Iborra, A.E. Escargueil, K.Y. Kwek, A. Akoulitchev, P.R. Cook, Molecular cross-talk between the transcription, translation, and nonsense-mediated decay machineries, J. Cell Sci. 117 (2004) 899–906.
[4] L.E. Maquat, Nonsense-mediated mRNA decay: splicing, translation and mRNP dynamics, Nat. Rev. 5 (2004) 89–99.
[5] L. Balvay, M.L. Lastra, B. Sargueil, J. Darlix, T. Ohlmann, Translational control of retroviruses, Nat. Rev. 5 (2007) 128–140.
[6] N.J. McGlincy, C.W. Smith, Alternative splicing resulting in nonsense-mediated mRNA decay: what is the meaning of nonsense? Trends Biochem. Sci. 33 (2008) 385–393.
[7] E.P. Plant, P. Wang, J.L. Jacobs, J.D. Dinman, A programmed-1 ribosomal frameshift signal can function as a *cis*-acting mRNA destabilizing element, Nucleic Acids Res. 32 (2004) 784–790.
[8] A.L. Saltzman, Y.K. Kim, Q. Pan, M.M. Fagnani, L.E. Maquat, B.J. Blencowe, Regulation of multiple core spliceosomal proteins by alternative splicing-coupled nonsense-mediated mRNA decay, Mol. Cell Biol. 28 (2008) 4320–4330.
[9] C. Theis, J. Reeder, R. Giegerich, KnotInFrame: prediction of -1 ribosomal frameshift events, Nucleic Acids Res. 36 (2008) 6013–6020.
[10] A.M. Dickson, J. Wilusz, Strategies for viral RNA stability: live long and prosper, Trends Genet. 27 (2011) 286–293.
[11] S. Boelz, G. Neu-Yilik, N.H. Gehring, M.W. Hentze, A.E. Kulozik, A chemiluminescence-based reporter system to monitor nonsense-mediated mRNA decay, Biochem. Biophys. Res. Commun. 349 (2006) 186–191.
[12] T. Ohsugi, T. Kumasaka, T. Urano, Construction of a full-length human T cell leukemia virus type I genome from MT-2 cells containing multiple defective proviruses using overlapping polymerase chain reaction, Anal. Biochem. 329 (2004) 281–288.
[13] N.H. Gehring, G. Neu-Yilik, T.W. Schell, M. Hentze, A.E. Kulozik, Y14 and hUpf3b form an NMD-activating complex, Mol. Cell 11 (2003) 939–949.
[14] Y.K. Kim, L. Furic, L. DesGroseillers, L.E. Maquat, Mammalian staufen1 recruits Upf1 to specific mRNA 3_UTRs so as to elicit mRNA decay, Cell 120 (2005) 195–208.
[15] B. Lee, Y. Tanaka, H. Tozawa, Monoclonal antibody defining Tax1 protein of human T-cell leukemia virus type-I, Tohoku J. Exp. Med. 157 (1989) 1–11.
[16] Y. Tanaka, B. Lee, T. Inoi, H. Tozawa, N. Yamamoto, Y. Hinuma, Antigens related to three core proteins of HTLV-I (p24, p19 and p15) and their intracellular localizations, as defined by monoclonal antibodies, Int. J. Cancer 37 (1986) 35–42.
[17] J. Zhao, B.K. Sun, J.A. Erwin, J. Song, J.T. Lee, Polycomb proteins targeted by a short repeat RNA to the mouse X chromosome, Science 322 (2008) 750–756.
[18] M. Gröne, C. Koch, R. Grassmann, The HTLV-1 Rex protein induces nuclear accumulation of unspliced viral RNA by avoiding intron excision and degradation, Virology 218 (1996) 316–325.
[19] M. Hidaka, J. Inoue, M. Yoshida, M. Seiki, Post-transcriptional regulator (rex) of HTLV-1 initiates expression of viral structural proteins but suppresses expression of regulatory proteins, EMBO J. 7 (1988) 519–523.
[20] J. Inoue, M. Yoshida, M. Seiki, Transcriptional (p40x) and post-transcriptional (p27x-III) regulators are required for the expression and replication of human T-cell leukemia virus type I genes, Proc. Natl. Acad. Sci. U. S. A. 84 (1987) 3653–3657.
[21] A. Eulalio, I. Behm-Ansmant, E. Izaurralde, P-Bodies: at the crossroads of post-transcriptional pathways, Nat. Rev. 8 (2007) 9–22.
[22] T.M. Franks, G. Singh, J. Lykke-Andersen, UPF1 ATPase dependent mRNP disassembly is required for completion of nonsense-mediated mRNA decay, Cell 143 (2010) 938–950.
[23] O. Isken, L.E. Maquat, The multiple lives of NMD factors: balancing roles in gene and genome regulation, Nat. Rev. 9 (2008) 699–712.
[24] R. Parker, U. Sheth, P bodies and the control of mRNA translation and degradation, Mol. Cell 25 (2007) 635–646.
[25] J. Rehwinkel, I. Behm-Ansmant, D. Gatfield, E. Izaurralde, A crucial role for GW182 and the DCP1:DCP2 decapping complex in miRNA-mediated gene silencing, RNA 11 (2005) 1640–1647.
[26] U. Sheth, R. Parker, Targeting of aberrant mRNAs to cytoplasmic processing bodies, Cell 125 (2006) 1095–1109.
[27] L. Unterholzner, E. Izaurralde, SMG7 acts as a molecular link between mRNA surveillance and mRNA decay, Mol. Cell 16 (2004) 587–596.
[28] J.E. Weil, K.L. Beemon, A 3′ UTR sequence stabilizes termination codons in the unspliced RNA of Rous sarcoma virus, RNA 12 (2007) 102–110.
[29] E.G. Lee, D. Kuppers, M. Horn, J. Roy, C. May, M.L. Linial, A premature termination codon mutation at the C terminus of foamy virus *gag* downregulates the levels of spliced *pol* mRNA, J. Virol. 82 (2008) 1656–1664.
[30] L. Ajamian, L. Abrahamyan, M. Milev, P.V. Ivanov, A.E. Kulozik, N.H. Gehring, A.J. Mouland, Unexpected roles for UPF1 in HIV-1 RNA metabolism and translation, RNA 14 (2008) 914–927.
[31] J.R. Hogg, S.P. Goff, UPF1 senses 3′ UTR length to potentiate mRNA decay, Cell 143 (2010) 379–389.
[32] O.U. Susova, V.E. Gurtsevich, The role of region pX in the life cycle of HTLV-I and in carcinogenesis, Mol. Biol. 37 (2003) 334–344.
[33] G. Franchini, R. Fukumoto, J.R. Fullen, T-cell control by human T-cell leukemia/lymphoma virus type-1, Int. J. Hematol. 78 (2003) 280–296.
[34] M. Boxus, J.-C. Twizere, S. Legros, J.-F. Dewulf, R. Kettmann, L. Willems, The HTLV-1 Tax interactome, Retrovirology 5 (2008) 76.

[35] F. Kashanchi, J.N. Brady, Transcriptional and post-transcriptional gene regulation of HTLV-1, Oncogene 24 (2005) 5938–5951.
[36] I. Younis, P.L. Green, The human T-cell leukemia virus Rex protein, Front. Biosci. 10 (2005) 431–445.
[37] C. Nicot, M. Dundr, J.M. Johnson, J.R. Fullen, N. Alonzo, R. Fukumoto, G.L. Princler, D. Derse, T. Misteli, G. Franchini, HTLV-1-encoded p30II is a post-transcriptional negative regulator of viral replication, Nat. Med. 10 (2004) 197–201.
[38] U. Sinha-Datta, A. Datta, S. Ghorbel, M. Duc Dodon, C. Nicot, Human T-cell lymphotrophic virus type I Rex and p30 interactions govern the switch between virus latency and replication, J. Biol. Chem. 282 (2007) 14608–14615.
[39] H.H. Baydoun, M. Bellon, C. Nicot, HTLV-1 yin and yang: Rex and p30 master regulators of viral mRNA trafficking, AIDS Rev. 10 (2008) 195–204.
[40] Y.F. Ahmed, G.M. Gilmartin, S.M. Hanly, J.R. Nevins, W.C. Greene, Structure–function analyses of the HTLV-I Rex and HIV-1 Rev RNA response elements: insights into the mechanism of Rex and Rev action, Gene Develop. 4 (1990) 1014–1022.
[41] Y.F. Ahmed, G.M. Gilmartin, S.M. Hanly, J.R. Nevins, W.C. Greene, The HTLV-I Rex response element mediates a novel form of mRNA polyadenylation, Cell 64 (1991) 727–737.
[42] Y. Adachi, T. Nosaka, M. Hatanaka, Protein kinase inhibitor H-7 blocks accumulation of unspliced mRNA of human T-cell leukemia virus type I (HTLV-I), Biochem. Biophys. Res. Commun. 169 (1990) 469–475.
[43] Y. Hakata, T. Umemoto, S. Matsushita, H. Shida, Involvement of human CRM1 (exportin 1) in the export and multimerization of the Rex protein of human T-cell leukemia virus type 1, J. Virol. 72 (1998) 6602–6607.
[44] Y. Hakata, M. Yamada, Rat CRM1 is responsible for the poor activity of human t-cell leukemia virus type 1 Rex protein in rat cells, J. Virol. 75 (2001) 11515–11525.
[45] V. Mocquet, J. Neusiedler, F. Rende, D. Cluet, J.-P. Robin, J.-M. Terme, M. Duc Dodon, J. Wittmann, C. Morris, H.L. Hir, V. Ciminale, P. Jalinot, The human t-lymphotropic virus type 1 Tax protein inhibits nonsense-mediated mRNA decay by interacting with INT6/EIF3E and UPF1, J. Virol. 86 (2012) 7530–7543.
[46] F. Rende, I. Cavallari, A. Corradin, M. Silic-Benussi, F. Toulza, G.M. Toffolo, Y. Tanaka, S. Jacobson, G.P. Taylor, D.M. D'Agostino, C.R.M. Bangham, V. Ciminale, Kinetics and intracellular compartmentalization of HTLV-1 gene expression: nuclear retention of HBZ mRNAs, Blood 117 (2011) 4855–4859.
[47] P. Nicholson, H. Yepiskoposyan, S. Metze, R.Z. Orozco, N. Kleinschmidt, O. Mühlemann, Nonsense-mediated mRNA decay in human cells: mechanistic insights, functions beyond quality control and the double-life of NMD factors, Cell. Mol. Life Sci. 67 (2010) 677–700.
[48] L.B. Gardner, Nonsense-mediated RNA decay regulation by cellular stress: implications for tumorigenesis, Mol. Cancer Res. 8 (2010) 295–308.

Carnosol, rosemary ingredient, induces apoptosis in adult T-cell leukemia/lymphoma cells via glutathione depletion: proteomic approach using fluorescent two-dimensional differential gel electrophoresis

Yo-ichi Ishida, Masao Yamasaki, Chizuko Yukizaki, Kazuo Nishiyama, Hirohito Tsubouchi, et al.

Human Cell

e-ISSN 1749-0774

Human Cell
DOI 10.1007/s13577-013-0083-6

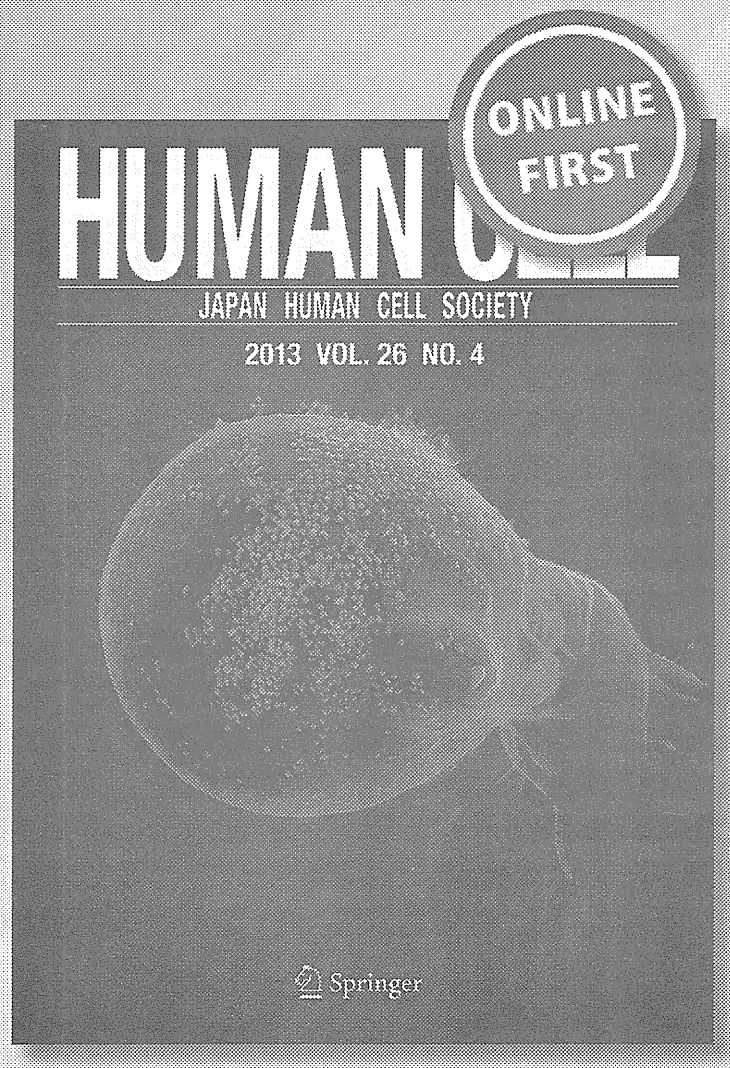

Springer

Human Cell
DOI 10.1007/s13577-013-0083-6

RESEARCH ARTICLE

Carnosol, rosemary ingredient, induces apoptosis in adult T-cell leukemia/lymphoma cells via glutathione depletion: proteomic approach using fluorescent two-dimensional differential gel electrophoresis

Yo-ichi Ishida · Masao Yamasaki · Chizuko Yukizaki · Kazuo Nishiyama · Hirohito Tsubouchi · Akihiko Okayama · Hiroaki Kataoka

Received: 9 September 2013 / Accepted: 7 October 2013

Abstract Adult T-cell leukemia/lymphoma (ATL) is a fatal malignancy caused by infection with human T-lymphotropic virus type-1 and there is no accepted curative therapy for ATL. We searched for biological active substances for the prevention and treatment of ATL from several species of herbs. The ATL cell growth-inhibitory activity and apoptosis assay showed that carnosol, which is an ingredient contained in rosemary (*Rosmarinus officinalis*), induced apoptosis in ATL cells. Next, to investigate the apoptosis-inducing mechanism of carnosol, we applied proteomic analysis using fluorescent two-dimensional differential gel electrophoresis and mass spectrometry. The proteomic analysis showed that the expression of reductases, enzymes in glycolytic pathway, and enzymes in pentose phosphate pathway was increased in carnosol-treated cells, compared with untreated cells. These results suggested that carnosol affected the redox status in the cells. Further, the quantitative analysis of glutathione, which plays the central role for the maintenance of intracellular redox status, indicated that carnosol caused the decrease of glutathione in the cells. Further, *N*-acetyl-L-cystein, which is precursor of glutathione, canceled the efficiency of carnosol. From these results, it was suggested that the apoptosis-inducing activity of carnosol in ATL cells was caused by the depletion of glutathione.

Keywords ATL · Rosemary · Carnosol · Apoptosis · Glutathione depletion

Introduction

Adult T-cell leukemia/lymphoma (ATL) is a fatal malignancy caused by infection with human T-lymphotropic virus type-1 (HTLV-1) [1]. Ten to twenty million people is infected worldwide with HTLV-1 and about 2.5–5 % of

Y. Ishida (✉)
Department of Biochemistry, Meiji Pharmaceutical University,
2-522-1 Noshio, Kiyose, Tokyo 204-8588, Japan
e-mail: ishida@my-pharm.ac.jp

Y. Ishida · A. Okayama
Miyazaki Prefectural Industrial Support Foundation,
16500-2 Higashi-Kaminaka, Sadowara-cho,
Miyazaki 880-0303, Japan

M. Yamasaki · K. Nishiyama
Department of Biochemistry and Applied Biosciences,
Faculty of Agriculture, University of Miyazaki,
1-1 Gakuenkibanadai-nishi, Miyazaki 889-2192, Japan

C. Yukizaki
Miyazaki Prefecture Food Research
and Development Center, 16500-2 Higashi-Kaminaka,
Sadowara-cho, Miyazaki 880-0303, Japan

H. Tsubouchi
Digestive Disease and Lifestyle-related
Disease Health Research, Human and Environmental Sciences,
Kagoshima University Graduate School of Medicine
and Dental Sciences, 8-35-1 Sakuragaoka,
Kagoshima 890-8544, Japan

A. Okayama
Division of Rheumatology, Infectious Diseases,
and Laboratory Medicine, Department of Internal Medicine,
Faculty of Medicine, University of Miyazaki, 5200 Kihara,
Kiyotake, Miyazaki 889-1692, Japan

H. Kataoka
Section of Oncopathology and Regenerative Biology,
Department of Pathology, Faculty of Medicine,
University of Miyazaki, 5200 Kihara, Kiyotake,
Miyazaki 889-1692, Japan

Published online: 10 December 2013

viral carriers develop ATL after a long latent period (30–50 years) [2]. Once developed, ATL has a poor prognosis with a mean survival time of 13 months, being refractory to currently available combination chemotherapy [3]. Although hematopoietic stem cell transplantation and molecular-targeted drugs have been also tried, there is at present no accepted curative therapy for ATL and the development of new therapeutic and preventive strategies is necessary [4]. Considering that only a part of viral carriers develops ATL after the long latent period, it is speculated that the onset of ATL is influenced by a diet taken daily in a similar manner to that of life-style-related diseases such as diabetes and cancers.

Functional foods and their ingredients are focused as natural resources for the prevention and treatment of life style-related diseases. For example, several polyphenols derived from various fruits and vegetables are suggested to be effective for cancer prevention [5, 6]. In ATL, several groups including us reported that epigallocatechin-3-gallate, capsaicin, and genistein, which are ingredients of green tea, red pepper, and soy, respectively, induce apoptosis in ATL cells and HTLV-1—infected cells [7–10]. These findings support the efficiency of functional foods and these ingredients against ATL and HTLV-1—infection. Thus, in this study, we focused on herbs and their ingredients as the other natural sources, because herbs have been used not only as food but also for medical purposes traditionally [11, 12]. It was found that carnosol, which is a polyphenol contained in rosemary (*Rosmarinus officinalis*), induced apoptosis in ATL cells.

Carnosol has been reported to have the apoptosis-inducing activity [13]; however, its action mechanism is not understood fully. Here, to clarify the mechanism of carnosol-induced apoptosis in ATL cells, we comprehensively examined proteins differentially expressed between the cells treated with the drug and untreated by proteomic analysis based on two-dimensional differential gel electrophoresis (2D-DIGE) and mass spectrometry (MS) [14]. Proteomic analysis of ATL cells suggested that carnosol affected the redox regulation in the cells. Thus, we next focused on glutathione, which plays the central role for the maintenance of intracellular redox status. From the quantitative analysis of glutathione and the experiment using its precursor *N*-acetyl-L-cysteine (NAC), it was suggested that the depletion of glutathione is a cause of carnosol-induced apoptosis in ATL cells.

Materials and methods

Reagents

Carnosol, NAC, and catalase were purchased from Cayman chemical (Ann Arbor, MI), Wako pure chemical industries (Osaka, Japan), and Sigma-Aldrich (St. Louis, MO), respectively.

Cell culture

ATL cell lines (ED and S1T cells), HTLV-1—infected cell line (MT-2 cells), and T-cell acute lymphoblastic leukemia cell line (Jurkat cells) were cultured in RPMI 1640 medium supplemented with 10 % fetal bovine serum. ED cells, S1T cells, and MT2 cells were kindly provided by Dr. Kazuhiro Morishita (Miyazaki University, Japan) [15].

Preparation of herbal extracts

Dried leaves of peppermint (*Mentha x piperita*), rosemary (*Rosmarinus officinalis*), spearmint (*Mentha spicata*), basil (*Ocimum basilicum*), or lemon balm (*Melissa officinalis*) were extracted with 80 % ethanol. After removal of insoluble materials by filtration, the solvent was evaporated. Dry residue was dissolved with dimethyl sulfoxide (DMSO) at the concentration of 200 mg/ml and stored at −20 °C until assay. Similarly, the extract of green tea (*Camellia sinensis*) was also prepared.

Cell viability assay

Briefly, 1×10^4 cells were seeded into a well of 96-well plates, cultured for 24 h, and then allowed to grow in the presence or absence of herbal extracts or carnosol. For the cells untreated with extracts or carnosol, a volume of DMSO equal to that used in the treated cells was added to the medium. After 72 h culture, 10 µl WST-8 (Dojindo Molecular Technologies, Kumamoto, Japan) was added to each well followed by 4 h incubation at 37 °C and then the absorbance of each well was measured at 450 nm with reference wavelength at 655 nm using an Emax Precision microplate reader (Molecular Devices Inc., Sunnyvale, CA). Cell viability was calculated as relative index of the untreated cells. Effects of herbal extracts on cell viability were expressed as the 50 % inhibitory concentration (IC50). Cell viability was also examined by trypan blue staining.

Antibodies

For the evaluation of apoptosis, anti-cleaved caspase-3 (Asp175) antibody (Cell Signaling Technology, Beverly, MA) and anti-cleaved caspase-7 (Asp198) antibody (Cell Signaling Technology) were used. Anti-moesin monoclonal antibody, a rabbit polyclonal IgG against annexin A1, and anti-actin monoclonal antibody were purchased from AbD Serotec (Oxford, UK), Aviva Systems Biology (San Diego, CA), and Sigma–Aldrich, respectively. Rabbit

polyclonal antibodies against α-enolase and thioredoxin reductase 1 were purchased from Santa Cruz Biotechnology, Inc. (Santa Cruz, CA). Horseradish peroxidase (HRP)-conjugated goat anti-rabbit and mouse immunoglobulins were purchased from Cappel Organon Teknika (West Chester, PA).

Apoptosis assay

Apoptotic cells were detected using the Human annexin V-fluorescein isothiocyanate (FITC) kit (Bender MedSystems, Vienna, Austria). The cells were stained with FITC-conjugated annexin V and propidium iodide (PI) followed by flow cytometric analysis with an EPICS XL flow cytometer (Beckman Coulter, Inc., Fullerton, CA). To detect activated caspases, the cells were extracted with a buffer containing 50 mM Tris–HCl (pH 7.4), 1 % Triton X-100, 150 mM NaCl, 1 mM EDTA, 50 mM NaF, 30 mM $Na_4P_2O_7$, and Protease inhibitor cocktail (Nacalai Tesque, Kyoto, Japan) and then western blotting using antibodies against cleaved caspases was performed.

Western blotting

The protocol for western blotting was modified from the previous report [16]. The samples were separated by sodium dodecyl sulfate (SDS)-polyacrylamide gel electrophoresis (PAGE) and then the proteins were transferred electrophoretically onto Immobilon-P transfer membranes (Millipore, Bedford, MA, USA). Membranes were blocked and then incubated with primary antibodies in solution 1 of Can Get Signal (Toyobo, Osaka, Japan) for 1 h at room temperature, followed by HRP-conjugated secondary antibodies in its solution 2 for 1 h at room temperature. As primary antibodies, anti-cleaved caspase-3 (Asp175), anti-cleaved caspase-7 (Asp198), and anti-moesin, anti-annexin A1 antibodies were used at 1:1000 dilution. Antibodies against α-enolase, thioredoxin reductase 1, and actin were used at 1:2000, 1:500, and 1:4000 dilutions, respectively. Secondary antibodies were used at 1:10000 dilution. The labeled proteins were visualized with an ECL Western Blotting Detection Reagents (GE Healthcare, Little Chalfont, UK). The band intensity of each protein was measured by NIH image.

Fluorescent 2D-DIGE

Fluorescent 2D-DIGE was performed as described previously [14]. Total cell extracts were obtained by homogenizing the cells harvested in 50 mM phosphate (pH 8) containing the complete protease inhibitor cocktail (Roche Diagnostics, Mannheim, Germany) with a polytron homogenizer (Ultra-Turrax T8, IKA-Werke, Staufen, Germany). Fifty microgram of total proteins from carnosol-treated or untreated cells were fluorescently labeled with IC5-OSu (excitation, 640 nm; emission, 660 nm). On the other hand, mixture of equal quantities of both samples was labeled with IC3-OSu (excitation, 550 nm; emission, 570 nm). IC3-OSu—and IC5-OSu—labeled samples were mixed together and then the first dimension isoelectric focusing (IEF) electrophoresis was performed using ReadyStrip IPG strips (pH 3–10 NL, 7 cm; Bio-Rad Laboratories) on Protean IEF cell (Bio-Rad Laboratories) followed by SDS-PAGE using 8 % gel for the second dimensional separation. Fluorescent 2D-DIGE images of IC3-OSu—and IC5-OSu—labeled samples were obtained using appropriate excitation/emission filters equipped on a Proxpress proteomic imaging system (PerkinElmer Life Sciences, Waltham, MA). Because IC3-OSu images obtained and fluorescent intensity of protein spots contained in them are to be theoretically identical between all gels, the IC3-OSu—labeled proteins serve as reference for spot matching and quantification of IC5-OSu—labeled proteins [14]. Thus, after all images were aligned based on IC3-OSu images using SameSpot TT900 S2S (Nonlinear Dynamics, Newcastle, UK), protein spot intensities in IC5-OSu images were calculated using Progenesis Discovery (Nonlinear Dynamics). Each group (carnosol-treated or untreated) was run on triplicate gels twice and the average spot intensities from total 6 gels were expressed as normalized volume ± standard deviation (SD). Statistical differences were determined by the Student t test. Values of $p < 0.05$ were considered significant.

Protein identification

Proteins expressed differentially were identified by in-gel digestion and peptide mass finger printing (PMF) using MS [14]. Briefly, gels were stained with coomassie brilliant blue R-250 and then spots of interest were cut off. The gel pieces were destained in 25 mM NH_4HCO_3 and 50 % acetonitrile and then incubated in reducing solution (25 mM NH_4HCO_3 and 10 mM dithiothreitol) for 1 h at 56 °C followed by further incubation for 45 min at room temperature in alkylation solution (25 mM NH_4HCO_3 and 55 mM iodoacetamide). After dehydrating with acetonitrile, the gel pieces were incubated overnight in digesting solution [50 mM NH_4HCO_3, 10 μg/ml trypsin (Trypsin Gold, mass spectrometry grade; Promega, Madison, WI), and 1 % n-octyl-β-D-glucoside (Dojindo Molecular Technologies)]. The peptides produced were extracted with extraction solution (50 % acetonitrile and 5 % trifluoroacetic acid) and then

spectra were obtained using matrix-assisted laser desorption/ionization (MALDI)-time of flight (TOF)-TOF–MS, Autoflex II TOF/TOF (Bruker Daltonics, Bremen, Germany). The data set was entered in an in-house Mascot search engine (Matrix Science, London, UK) to find the closest match with known proteins registered in the database from the Swiss-Prot.

Glutathione assay

Level of intracellular glutathione (reduced form, GSH; oxidized form, GSSG) was examined using Bioxytech GSH/GSSG-412 assay kit (OxisResearch, Portland, OR). Data were calculated based on standard curves created with known amounts of GSH and expressed as the

Table 1 Leukemia cell growth-inhibitory activity in 80 % ethanol extracts of several herbal species

Herbal species		IC50 value (μg/ml)			
Common name	Botanical name	ED	S1T	MT-2	Jurkat
Green tea	*Camellia sinensis*	204	261	301	284
Peppermint	*Mentha x piperita*	32.5	40.9	56.8	25.1
Rosemary	*Rosmarinus officinalis*	20.6	44.4	22.0	16.7
Spearmint	*Mentha spicata*	43.2	51.3	57.8	46.0
Basil	*Ocimum basilicum*	83.6	47.0	94.2	72.1
Lemon balm	*Melissa officinalis*	303	248	263	366

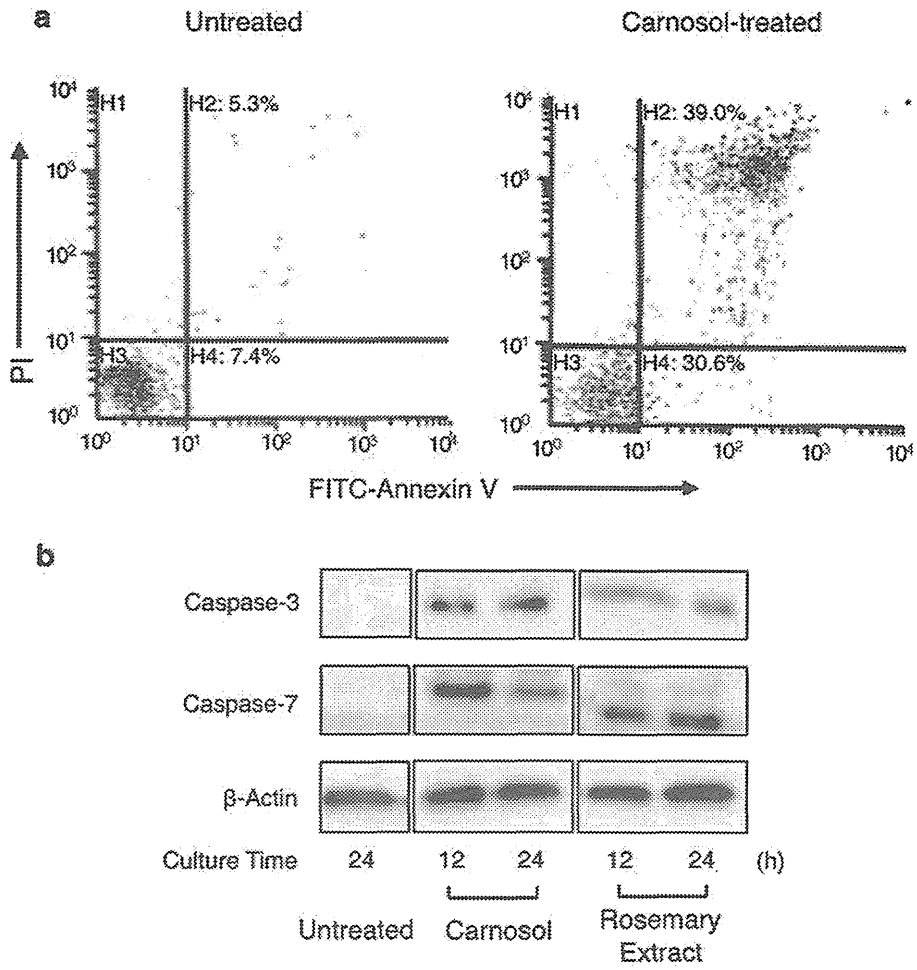

Fig. 1 Carnosol, a rosemary ingredient, induces apoptosis in ATL cells. ED cells were untreated or treated with 40 μM carnosol and then double-stained with PI and FITC-annexin V followed by flow cytometry (**a**). Annexin V-positive cells were increased by carnosol treatment. The activated forms of caspase-3 and caspase-7 were detected by western blotting (**b**)

amount per mg of protein. The ratio of GSH/GSSG was calculated from values of GSH and GSSG. Statistical differences were determined by the Student t test and values of $p < 0.05$ were considered significant.

Results

Rosemary extract and its ingredient, carnosol, induce apoptosis in ATL cells

To screen biological active substances for the prevention and treatment of ATL from herbs, ATL cell growth-inhibitory activity of 5 herbal extracts was examined by WST-8 (Table 1). In ED cells and S1T cells as ATL cell lines, IC50 values of 4 spices (peppermint, rosemary, spearmint, and basil) were lower than that of green tea, which has been reported to be effective for ATL. Similar results were obtained in MT2 cells and Jurkat cells as HTLV-1—infected cells and the other T-cell leukemia cells, respectively. Especially, rosemary extract showed the superior inhibitory activity.

Carnosol is an ingredient of rosemary and a polyphenolic compound having antioxidant activity [17]. To investigate a contributory ingredient present in rosemary extract and its inhibitory form, it was next examined whether carnosol induces apoptosis in ATL cells (Fig. 1). In ED cells treated with carnosol, the annexin V-stained cells were clearly increased, compared with untreated cells (Fig. 1a). Activated caspase-3 and caspase-7, which are both executioners of apoptotic program, were also detected (Fig. 1b). In the cells treated with rosemary extract, we failed to detect the stained cells specifically, maybe owing to the disturbance of staining by some fluorescent substance in the extract (data not shown); however, activated caspases were detected (Fig. 1b). These results suggested that carnosol is a contributory ingredient in ATL cell apoptosis-inducing activity of rosemary.

Investigation of apoptosis-inducing mechanism by proteomic analysis

Proteomic analysis is the powerful tool for clarifying the action mechanism of drugs [14, 18]. Thus, to investigate the mechanism of carnosol-induced apoptosis in ATL cells, ED cells treated with carnosol were subjected to proteomic analysis using fluorescent 2D-DIGE and MS. Proteins extracted from carnosol-treated cells and untreated cells were separated by fluorescent 2D-DIGE and protein spots differentially expressed were examined. Although the spots discernibly different were not found by visual contact of 2D-DIGE images, quantitative analysis revealed that the intensities of 17 spots and 6 spots were significantly increased (Nos. 1–17; arrows in Fig. 2) and decreased (Nos. 18–23; arrowheads in Fig. 2), respectively, in carnosol-

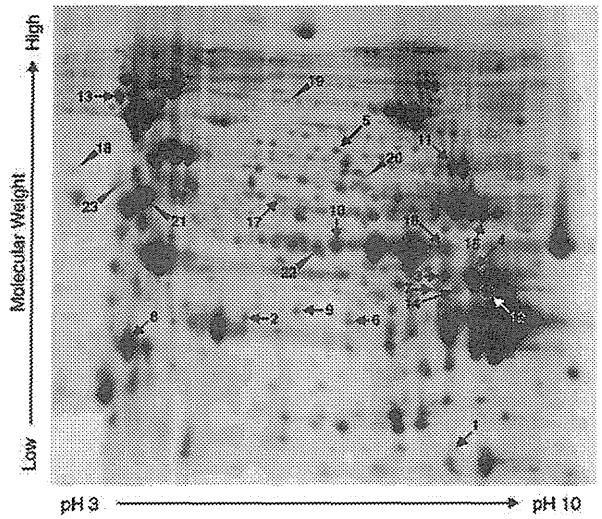

Fig. 2 Protein spots differentially expressed in carnosol-treated ED cells. Protein extracts from the cells that were untreated or treated with 40 μM carnosol for 24 h were fluorescent-labeled and then separated by 2D-DIGE followed by detection of protein spots with fluorescent imager. The fluorescent intensities of detected spots were calculated using Progenesis Discovery software. The image shows a representative pattern of IC3-OSu—labeled proteins as reference sample. In carnosol-treated cells, the spot intensities of 17 spots (Nos. 1–17; *arrows*) were increased as compared with untreated cells. In contrast, those of 6 spots (Nos. 18–23; *arrowheads*) were decreased. *Spot numbers* correspond to those in Table 2

treated cells as compared with untreated cells ($p < 0.05$; 1.3-fold change as cut off). Table 2 shows quantitative values of these spots. Next, proteins derived from these spots were identified by in-gel digestion and PMF using MALDI-TOF-TOF–MS (Table 2). These expression differences of our selected 4 proteins were also confirmed with western blotting (Fig. 3). From the list of proteins whose expression was increased by carnosol (Table 2), we found that these proteins fell mainly into three categories. The first is NADPH-dependent reductases (No. 1, flavin reductase; No. 9, biliverdin reductase A; No. 17, thioredoxin reductase 1). The second is enzymes in glycolytic pathway (Nos. 3 and 4, phosphoglycerate kinase 1; Nos. 10 and 16, α-enolase; No. 12, fructose-bisphosphate aldolase A; No. 15, glucose-6-phosphate isomerase). Although the same proteins were identified from multiple protein spots, this may be due to the post-translational modification and protein processing. The third is enzymes in pentose phosphate pathway (No. 2, transaldolase; No. 11, transketolase). The increase of expression of reductases implies the change of redox-status in the cells treated with carnosol. Moreover, these reductases were NADPH-dependent. Glycolytic and pentose phosphate pathways cooperate to contribute to the production of NADPH [19]. Consequently, it appeared that apoptosis-inducing activity of carnosol is related with NADPH-dependent redox regulation in the cells.

Table 2 Proteins expressed differentially in carnosol-treated ED cells

Spot no.[a]	Spot intensity[b]		Fold change[c]	p value[d]	Protein name[e]	Accession no.[f]	Sequence coverage (%)[g]	MW (kDa)[h]	pI[i]	Protein function[j]
	Untreated	Carnosol								
Increased										
1	1.07 ± 0.35	6.58 ± 4.22	6.16	0.025	Flavin reductase	P30043	28.8	22.1	7.3	NADPH-dependent reductase
2	0.69 ± 0.13	1.53 ± 2.22	2.22	0.011	Transaldolase	P37837	13.9	37.7	6.4	Regulation of pentose-phosphate pathway
3	1.06 ± 0.17	1.69 ± 0.22	1.60	2.5×10^{-4}	Phosphoglycerate kinase 1	P00558	24.8	44.9	8.3	Glycolytic enzyme
4	1.05 ± 0.12	1.66 ± 0.05	1.59	4.9×10^{-7}	Phosphoglycerate kinase 1	P00558	22.1	44.9	8.3	Glycolytic enzyme
5	0.68 ± 0.09	1.03 ± 0.06	1.51	1.2×10^{-5}	Moesin	P26038	18.6	67.8	6.1	Connection of cytoskeleton to the plasma membrane
6	0.76 ± 0.12	1.14 ± 0.08	1.49	8.1×10^{-5}	Annexin A1	P04083	23.8	38.8	6.6	Promotion of membrane fusion in exocytosis
7	0.77 ± 0.11	1.14 ± 0.34	1.48	0.044	26S protease regulatory subunit 10B	P62333	22.6	44.4	7.1	Component of 26S proteasome
8	1.00 ± 0.18	1.44 ± 0.12	1.44	5.6×10^{-4}	Annexin A5	P08758	46.4	35.8	4.9	Anticoaglant in blood coagulation cascade
9	1.00 ± 0.21	1.43 ± 0.32	1.43	0.020	Biliverdin reductase A	P53004	22.0	34.0	6.1	NADH- or NADPH-dependent reductase
10	1.08 ± 0.22	1.51 ± 0.35	1.40	0.029	α-Enolase	P06733	32.6	47.4	7.0	Glycolytic enzyme
11	0.77 ± 0.08	1.08 ± 0.20	1.39	0.006	Transketolase	P29401	12.7	68.5	7.6	Regulation of pentose-phosphate pathway
12	1.04 ± 0.20	1.42 ± 0.17	1.37	0.005	Fructose-bisphosphate aldolase A	P04075	26.2	39.7	8.4	Glycolytic enzyme
13	0.69 ± 0.08	0.95 ± 0.19	1.37	0.012	Endoplasmin	P14625	15.7	92.7	4.8	Molecular chaperone
14	0.95 ± 0.08	1.28 ± 0.21	1.35	0.010	Casein kinase II subunit α	P68400	23.0	45.2	7.3	Signal transduction
15	0.89 ± 0.09	1.18 ± 0.04	1.33	3.5×10^{-5}	Glucose-6-phosphate isomerase	P06744	16.7	63.2	9.1	Glycolytic enzyme
16	0.94 ± 0.04	1.25 ± 0.10	1.33	4.3×10^{-5}	α-Enolase	P06733	30.3	47.4	7.0	Glycolytic enzyme
17	0.80 ± 0.20	1.06 ± 0.03	1.32	0.023	Thioredoxin reductase 1	Q16881	15.4	55.5	6.1	NADPH-dependent reductase
Decreased										
18	1.46 ± 0.68	0.47 ± 0.18	−3.13	0.018	Nuclear autoantigenic sperm protein	P49321	12.4	85.5	4.3	DNA replication
19	0.78 ± 0.17	0.41 ± 0.14	−1.89	0.002	Methionine-tRNA ligase	P56192	9.30	102.2	5.8	Methionylation of tRNA
20	0.88 ± 0.24	0.64 ± 0.04	−1.38	0.040	Stress-induced-phosphoprotein 1	P31948	13.1	63.2	6.4	Mediation of association of HSC70 and HSP90
21	0.95 ± 0.05	0.71 ± 0.12	−1.34	0.001	Tubulin α-1C chain	Q9BQE3	24.3	50.5	5.0	Major constituent of microtubules
22	1.27 ± 0.06	0.94 ± 0.15	−1.34	6.4×10^{-4}	Elongation factor 1-γ	P26641	17.0	50.3	6.3	Elongation of translation
23	0.71 ± 0.09	0.53 ± 0.05	−1.33	0.002	Protein disulfide-isomerase	P07237	16.7	57.5	4.8	Formation of disulfide bonds

[a] Spot numbers correspond to those in Fig. 2

[b] Intensities of spots are shown as normalized volume ± SD (6 gels per group; untreated and carnosol-treated)

[c] Fold changes were calculated using Progenesis Discovery software and expressed as differences of spot intensities in carnosol-treated cells compared with those in untreated cells

[d] Statistical differences were determined by the Student t test. Values of $p < 0.05$ were considered significant

[e] Proteins were indentified using MASCOT with Swiss-Prot database

[f] References for the identified proteins

[g] Percentage cover of the identified peptides in total tryptic digests

[h] Theoretical molecular weight (MW) from MASCOT search results

[i] Theoretical isoelectric point (pI) from MASCOT search results

[j] The informations about protein functions were obtained by access using accession number from Swiss–Prot knowledgebase

Carnosol-induced apoptosis is caused by glutathione depletion but not extracellular H_2O_2

Glutathione is required for the maintenance of redox-status and plays a central role as antioxidant in the protection against oxidative stress through the cycling of GSH (reduced form) and GSSG (oxidized) [20, 21]. Further, the cycle is regulated by glutathione reductase and its enzymic activity is dependent on NADPH. Thus, to examine the relationship of glutathione to carnosol-induced apoptosis, the amounts of intracellular GSH and GSSG were quantified by commercially available kit (Fig. 4). Amounts of both

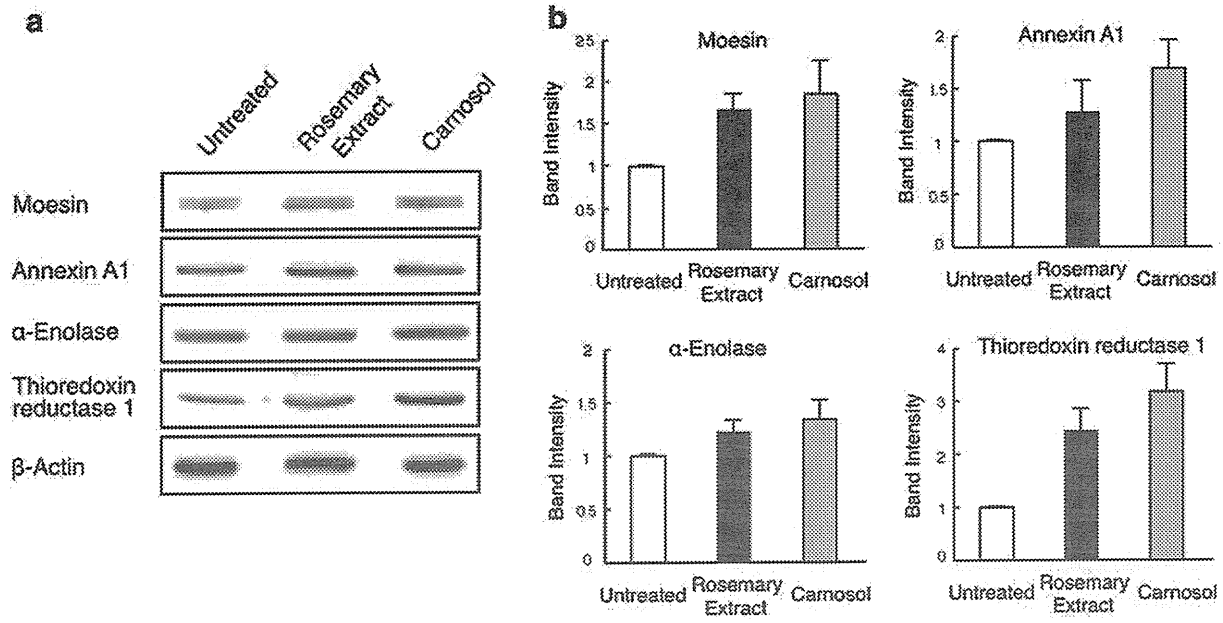

Fig. 3 Confirmation of expression of several identified proteins by western blotting. Protein extracts from the cells that were untreated or treated with 40 mg/ml rosemary extract or 40 μM carnosol for 24 h were electrophoresed and then blotted with antibody against moesin, annexin A1, α-enolase, thioredoxin reductase 1, or β-actin (**a**). The band intensity of each protein was measured by NIH image (**b**). The expression of these proteins was increased in carnosol-treated cells. Data represent the mean ± SD from three experiments

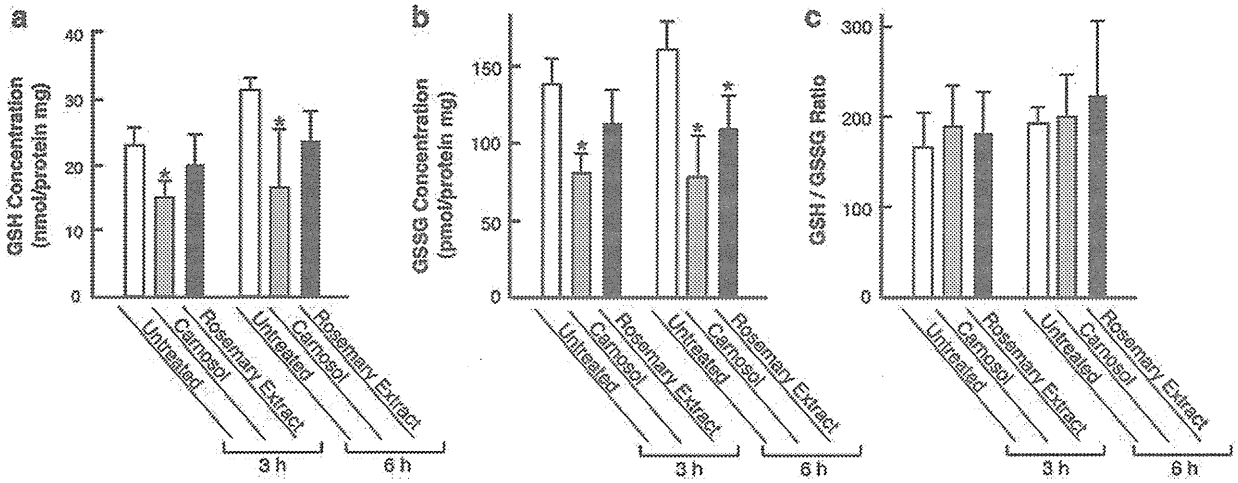

Fig. 4 Low level of intracellular glutathione in carnosol-treated ATL cells. ED cells were untreated (*white columns*) or treated with 40 μM carnosol (*gray columns*) or rosemary extract (*black columns*) for 3 or 6 h. Then intracellular GSH concentration (**a**), GSSG concentration (**b**), and GSH/GSSG ratio (**c**) were examined with GSH/GSSG assay kit. In carnosol-treated cells, the levels of GSH (*gray columns* in **a**) and GSSG (*gray columns* in **b**) were significantly lower as compared with the untreated cells (*white columns* in **a** and **b**). Data represent the mean ± SD from three experiments. * $p < 0.05$ (vs. untreated)

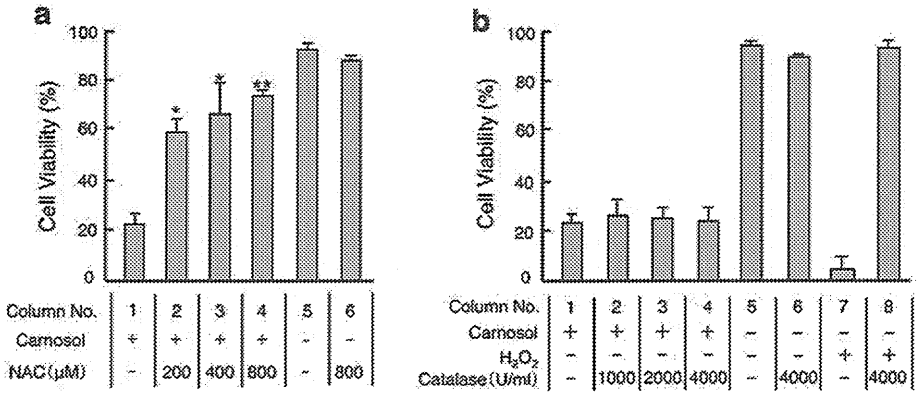

Fig. 5 Effects of exogenous NAC and catalase on efficiency of carnosol. ED cells were un-pretreated or pretreated with indicated concentrations of NAC (**a**) or catalase (**b**), and then 40 μM carnosol, equal volume of vehicle (DMSO), or 40 μM H_2O_2 was further added to media. After culture for 48 h, cell viability was examined by trypan blue staining. While cell viability was decreased by carnosol, it was restored dose-dependently by NAC (**a**) but not catalase (**b**). Data represent the mean ± SD from three experiments. * $p < 0.01$, ** $p < 0.001$ (columns 2–4 vs. column 1)

GSH and GSSG were significantly decreased in carnosol-treated cells as compared to untreated cells (white and gray columns in Fig. 4a, b). Also, in the cells treated with rosemary extract, they tended to be decreased (black columns in Fig. 4a, b). Meanwhile, the ratio of GSH and GSSG was not affected by carnosol (gray columns in Fig. 4c). These results indicated that the decrease of GSH in carnosol-treated cells was due to depletion of glutathione (both of GSH and GSSG), but not the acceleration of the oxidation of GSH to GSSG. Further to confirm the relationship of glutathione depletion, NAC, which is precursor of glutathione and used for the exogenous supplementation [21], was added to culture media of carnosol-treated ED cells (Fig. 5a). Cell viability was restored by NAC in dose-dependent manner (columns 2–4 in Fig. 5a). From these results, it was suggested that the apoptosis-inducing activity of carnosol in ATL cells was caused by the depletion of glutathione.

Apoptosis induced by polyphenols has been reported to be associated with the production of hydrogen peroxide (H_2O_2) in culture media by themselves [22, 23], suggesting that the efficiency may be artifact. Finally, we investigated whether the production of H_2O_2 in culture media is associated to apoptosis-inducing activity of carnosol or not, using catalase, a scavenger of H_2O_2 (Fig. 5b). In carnosol-treated cells, catalase addition did not restore the viability (columns 2–4 in Fig. 5b). The efficiency of carnosol was kept unchanged under the condition that extracellular H_2O_2 was scavenged by catalase. This suggests that carnosol does not act to the cells indirectly via H_2O_2 produced by itself.

Discussion

There has been increased interest in using herbs for the prevention and treatment of cancer [11, 12]. Many studies have reported the efficiency of herbs and their ingredients in various cancers [24, 25]. In this study, we found that rosemary extract and its ingredient carnosol have the activity that induces apoptosis in ATL cells and both action mechanisms are similar in the caspase activation, protein expression, and intracellular glutathione level. This suggests that carnosol is a contributory ingredient in ATL cell growth-inhibitory activity of rosemary, although possibilities of other ingredients such as carnosic acid and rosmarinic acid are still remained [17]. While this study is the first report on apoptosis-inducing activity of carnosol in ATL cells, the activity and cell cycle arrest have been also reported in the other cancer cells [13, 26, 27]. This suggests that the efficiency of carnosol is not specific to ATL, but common in various cancers. However, because this study is limited to the cell line analysis, the therapeutic efficacy and action mechanism of carnosol also need to be examined in xenograft animal models of ATL.

It is of interest why carnosol induced apoptosis in ATL cells. A depletion of intracellular glutathione has been described in a number of different apoptotic systems, with several studies showing that the depletion is the result of accelerated efflux rather than oxidation of GSH [28, 29]. In our system, glutathione depletion occurred in the cells treated with carnosol for short time of only 3 h. This rapid depletion implies the accelerated efflux of glutathione. Although it is still unclear how molecular mechanisms are present between carnosol and the efflux, the over-expression of Bcl-2, anti-apoptotic protein, has been reported to increase intracellular glutathione by suppressing the efflux from the cells [30]. Examining the relationship between carnosol and Bcl-2 might be necessary.

Living cells are always producing reactive oxygen species (ROS) such as H_2O_2 endogenously by the vital activity [29]. Glutathione prevents the oxidation of